Delay Time Correlation of Pressure Fluctuation Signals in the Novel Circulating Jet Tank

H.-B. Meng, F. Wang, Y.-F. Yu,* W. Wang, and J.-H. Wu
School of Energy and Power Engineering,
Shenyang University of Chemical Technology

Original scientific paper
Received: September 3, 2012
Accepted: April 19, 2013

In order to quantitatively evaluate the multiscale corrections of instantaneous flow in the novel circulating jet tank, the instantaneous pressure fluctuation signals (PFS) are measured by a data acquisition system. The original PFS are decomposed into seven uniform frequency bands from 0 to 70 Hz and a much wider frequency band from 70 to 250 Hz. The linear and nonlinear correlation characteristics of PFS under different circumferential angles and frequency bands are evaluated with autocorrelation and mutual information functions, respectively. With the increasing time delays, the autocorrelation of the original PFS decreases quickly and then fluctuates near zero. The fluctuations amplitudes, linear and nonlinear correlations decrease as the lower limits of decomposition frequency bands increase. The experimental results indicate that the signals of more than 50 Hz in frequency have no linear correlation, and there are no nonlinear and linear correlations for the time series signals, which are over 60 Hz in frequency.

Key words:
Circulating jet tank, mutual information function, autocorrelation, pressure fluctuation

Introduction

Jet mixers serve as one of the simplest devices to achieve mixing. In jet mixing, a part of the liquid in the tank is drawn through a pump and returned as a high-velocity jet through a nozzle into the tank. This jet entrains some of the surrounding liquid and creates a circulation pattern within the vessel thus leading to mixing of the contents.[1–2] By comparison to the traditional mechanical agitators, jet mixers are widely used in the processing industry and have some advantages such as high efficiency, low energy consumption, no moving parts, and so on.[3–4]

As far as the jet mixing performances were concerned, many researchers focused on the mixing time, flow characteristics and heat transfer, etc. Zughbi and Rakib[5] simulated various mixing vessel configurations and showed that minimizing the low velocity or dead zones reduced the mixing time. Hassel et al.[6] performed LES and three RANS models to predict averaged flow characteristics with different closure models in a coaxial jet mixer and compared with LIF and LDV measurements. Dong et al.[7] studied the flow and heat transfer characteristics of an impinging inverse diffusion flame jet, and four types of impinging flame structures had been identified and reported. The influences of the global equivalence ratio, Reynolds number of the air jet and the non-dimensional burner-to-plate distance on the flame structure, the local and averaged heat transfer characteristics were reported and discussed. Icardi et al.[8] employed micro-PIV and Direct Numerical Simulations to study the main mixing mechanisms in a confined impinging jet. With the help of CFD modeling, Patkar and Patwardhan[1] investigated the jet mixing of gases in cross-flow for various jet angles (30°, 45° downstream, 90° and 45° upstream) and different orifice shapes. Nunes et al.[9] assessed the micromixing performance of high viscosity fluids in the mixing chamber of a RIM machine.

A Circulating Jet Tank (CJT), as a novel unit operation for mixing, has effectively improved flow structures in tank and exhibits outstanding performance in the chemical field relative to the conventional mixer.[10–12] The principle of the CJT is to generate multiple jets with high velocity which entrain the surrounding fluids and create a composed circulatory pattern. The steady flow characteristics in the CJT were investigated using CFD method.[11–13]

An attractive option to study the instantaneous hydrodynamics of CJT is the analysis of pressure fluctuation signals (PFS).[14–15] The measuring method is well developed and relatively cheap. Furthermore, it is robust and therefore has great potential for use in industrial conditions. Studies on pressure fluctuations in reactors have been carried out for several years.[16–19] Fan et al.[20] characterized the flow regimes in a fluidized bed by the statistical proper-

*Correspondence: School of Energy and Power Engineering, Shenyang University of Chemical Technology, Shenyang 110142, Liaoning Province, P R China; Email address: taroyy@163.com

ties of the wall pressure fluctuations, especially the power spectral density function and the root mean square of the pressure fluctuations. Fan et al.[21] firstly studied pressure fluctuations in a gas-liquid-solid fluidized bed under different batch operating conditions by Hurst's rescaled range analysis. Vial et al.[22] found that the kurtosis of PFS exhibited a pronounced maximum at transition point from homogeneous to heterogeneous regime in bubble column or airlift reactor. Hu et al.[18] figured out the correlation integral of the pressure signals in the gas-liquid-solid slurry column and evaluated the maximum Lyapunov exponent. Ommen et al.[23] reviewed time series analysis methods for the dynamics of gas-solid fluidized beds at different fluidization regimes.

However, due to the defects of statistical methods mentioned above, the internal intrinsic information of the fluctuation signals could not be captured. Therefore, the linear analytical methods were put forward, such as the coherence function, transfer function based on the FFT transform, autocorrelation analysis and mutual correlation method. The linear analysis played a major role in fully understanding the frequency structure of the PFS.[14–15] But the methods mentioned above were not enough to reveal the non-homogeneity of the fluid flow system. In recent decades, nonlinear science has made great progress and many nonlinear techniques such as chaos theory, fractal, and information theory, have been used to study the dynamic evolution in time and space phase.[14–23]

The unsteady flow in the CJT still lacks systematic study and discussion. In this paper, the experiment is applied to measure the time series of instantaneous PFS at different spatial positions and different Reynolds numbers. PFS collected by sensors are generally contaminated in the process of data acquisition and transmission. In addition, the noise could seriously influence the result and precision of the nonlinear analysis. Based on frequency analysis with FFT, the PFS are decomposed into seven uniform frequency bands from 0 to 70 Hz and a much wider frequency band from 70 to 250 Hz. The distributions of autocorrelation and mutual information functions are evaluated respectively. The linear and nonlinear frequency ranges are proposed and the frequency band of fluctuation noise is determined.

Time delay correlation analysis

Generally speaking, a completely random noise signal has no linear correlation and nonlinear correlation at any delay time τ. Autocorrelation function describes the linear correlation of two variables between $x(i)$ and $x(i+\tau)$. The two different PFS are linearly independent when the first zero in their autocorrelation function is approached at a time delay τ_a. An important guide to the persistence in a time series is given by the series of quantities called the sample autocorrelation coefficients, which measure the correlation between observations at different times. The set of autocorrelation coefficients arranged as a function of separation in time is the sample autocorrelation function.[24] The autocorrelation function of PFS $x(i)$ is given by

$$R(\tau) = \frac{C_\tau}{\sigma_i \cdot \sigma_{i+\tau}} \tag{1}$$

where σ_i and $\sigma_{i+\tau}$ are standard deviations of the time series $x(i)$ and $x(i+\tau)$, respectively. The sample covariance C_τ is defined as:

$$C_\tau = \frac{1}{N-\tau}\sum_{i=1}^{N-\tau}\left(x_i - \overline{x}_i\right)\left(x_{i+\tau} - \overline{x}_{i+\tau}\right) \tag{2}$$

where N denotes the length of PFS.

Mutual information theory is widely used to ascertain time delay for reconstructing phase space. Mutual information function is a measure of the amount of information one random variable contains about another.[24–25] If the two variables are independent, the result of mutual information function between them is zero. If the two are strongly dependent, e.g., one variable is a function of the other variable, the value of mutual information function is large. Fraser and Swinney[26] first proposed that the value of time delays τ_m should be chosen as the first local minimum of mutual information. At the same time, the chaotic attractors can be adequately unfolded because of the least correlation between $x(i)$ and $x(i+\tau)$. The mutual information function between them can be expressed as follows[27]

$$\begin{aligned} I(x(i), x(i+\tau)) &= H(x(i+\tau)) + H(x(i)) - H(x(i+\tau), x(i)) \\ &= \sum_{i=1}^{N-\tau} P(x(i), x(i+\tau)) \ln P(x(i), x(i+\tau)) - \\ &\quad - \sum_{i=1}^{N-\tau} P(x(i)) \ln P(x(i)) - \\ &\quad - \sum_{i=1}^{N-\tau} P(x(i+\tau)) \ln P(x(i+\tau)) \end{aligned} \tag{3}$$

where $H(x(i))$ and $H(x(i+\tau))$ are the entropy of $x(i)$ and $x(i+\tau)$, respectively. $H(x(i), x(i+\tau))$ is the mutual entropy between $x(i)$ and $x(i+\tau)$. $P(x(i))$ is the probability distribution of $x(i)$. $P(x(i), x(i+\tau))$ is the joint probability between $x(i)$ and $x(i+\tau)$.

Experiments

Experimental apparatus

The experimental apparatus included a laboratory-scale CJT and a data acquisition system as shown in Fig. 1. The on-line dynamic data acquisitions were implemented based on dynamic signal collector Dewe-3021 and five dynamic pressure sensors DYG32000. A WILO MHI802 centrifugal pump was used to withdraw fluid from the downcomer and pump it through the inlet pipe to the jet nozzles, where the fluid was ejected into the tank as the high-speed jet stream.

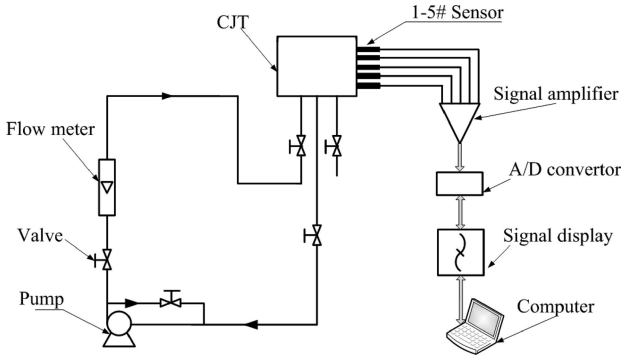

Fig. 1 – *Schematic diagram of experimental set-up for instantaneous PFS*

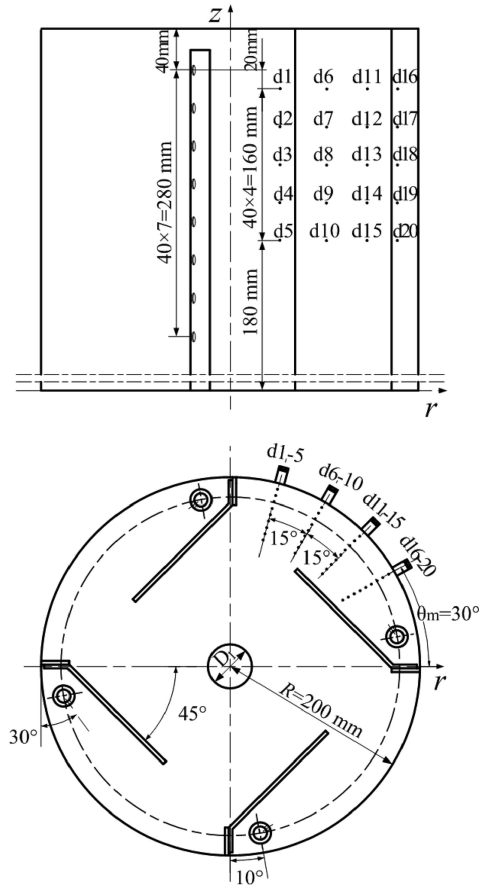

Fig. 2 – *Locations of measurement points for instantaneous PFS*

The CJT was 0.4 m in diameter and 0.5 m in height. The jet mixing tank with a flat bottom was equipped with four straight baffles. The origin of the cylindrical coordinate system was centered on the bottom of the CJT, where the *r*-axis and *z*-axis were in horizontal and axial directions, respectively. The angle between straight baffles and tank tangent was 45˚. The other parameters of the CJT and fluid properties for experiment are described in Fig. 2.

Measurement conditions

PFS measurements were conducted in the quarter of CJT. Distilled water was employed as the circulating working medium to ensure the sensitivity of the sensors. Pressure sensors and measurement points used in this study have been described in detail in our earlier study.[28] The circulating condition was evaluated by Reynolds numbers at the outlet of the nozzles. Considering the pressure drop along the risers induced by the adjacent nozzle spaces, the multiple nozzles work independently and have different jet velocities. As a result, it is necessary to employ an average velocity of jet flow, which can be derived from the conservation of mass.

$$u_m = \frac{4Q}{N_0 \pi d_j^2} \tag{4}$$

Standard deviation distributions of PFS at different ratios of d_j/R have been discussed by Yu et al.[29] So, in this paper we chose d_j as the characteristic length to evaluate the Reynolds number with the optimized ratio $d_j/R = 0.025$. Therefore, the average Reynolds number in the jet nozzles can be defined as,

$$Re = \frac{160\rho Q}{\pi \mu R N_0} \tag{5}$$

where Q, ρ, N_0, R and μ denote the volumetric flow rate passing through the flow meter, the density of fluid, the number of jet nozzles, the radius of tank, and the viscosity of fluid, respectively. The volumetric flow rate monitored by metallic rotor flow meter LZD-50/Y10/RR1/ESK was in the range of 1–9 m^3 h^{-1}. As a result, the Reynolds numbers were greater than 30 to ensure fully turbulent flow in all cases (*Re* from 3660 to 32940). The sampling frequency was 250 Hz, satisfying the Nyquist-Shannon sampling theorem. The pressure fluctuation time series with a duration of 132 s were measured. Each of the three data sets contained a little over 33 000 data points.

Results and discussion

Because the start and termination of PFS were subject to noise contamination, we intercepted the middle data as the single variable time series.[30] In

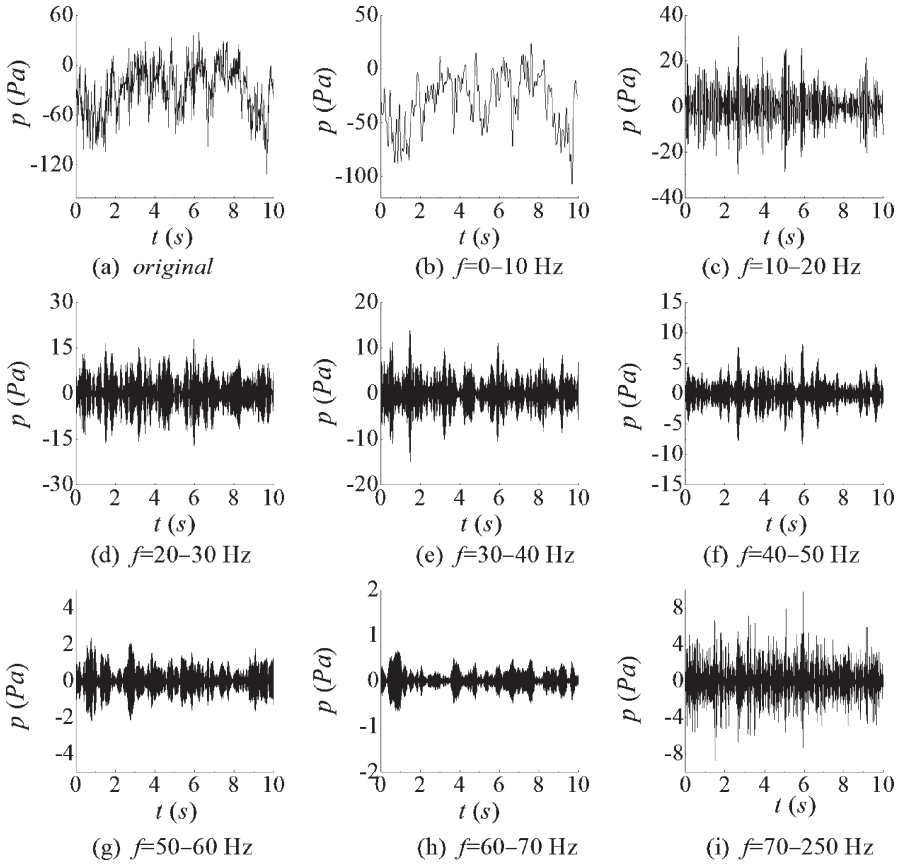

Fig. 3 – *Decomposed time series of different frequency bands based on Fourier method*

order to extract as much dynamic characteristics of time series as possible, we selected $N_1 = 30000$ as the optimal set length.

PFS decomposition

The noises perhaps exist in the time series of pressure fluctuation and are induced by the fluctuation of operating condition, the rotation of the pump impellers and analog-to-digital conversion process. The noises embedded in PFS are almost high frequency signals, which have a negative impact on the reconstruction of chaotic attractors. Therefore, the real signals must be filtered in frequency, that is, the signals in the given frequency domain can be blocked or passed.

The original time series of PFS at $r/R = 0.825$ of d16 and $Re = 29280$ is decomposed into eight subbands in frequency by Fourier time-frequency filter: 0–10 Hz, 10–20 Hz, 20–30 Hz, 30–40 Hz, 40–50 Hz, 50–60 Hz, 60–70 Hz and 70–250 Hz. Then the instantaneous PFS components with distinguishing frequency bands are obtained by inverse FFT as shown in Fig. 3(b)-(i). It could be seen from the figure that the signals are more disordered and their fluctuation amplitudes are smaller with the increasing decomposition frequency. That is, the energy ratios of PFS with high frequency bands are lower than the large-scale fluctuation signals and the main frequency mainly remains in low frequency below 10 Hz. That is in good agreement with the analysis of Hilbert spectrum.[28] The large-scale fluctuation signals of the instantaneous pressure in the CJT are low frequency signals.

Fig. 4 describes the comparison of autocorrelation functions between PFS and white noise. The results show that white noise is entirely random and the autocorrelation function is almost zero, while the autocorrelation function of the PFS decreases quickly and then fluctuates near zero with the increase in the time delays. This means that PFS have

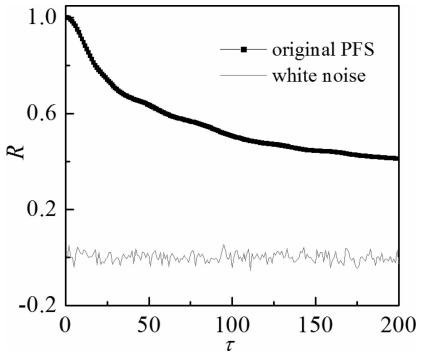

Fig. 4 – *Autocorrelation functions of the original PFS and white noise signal*

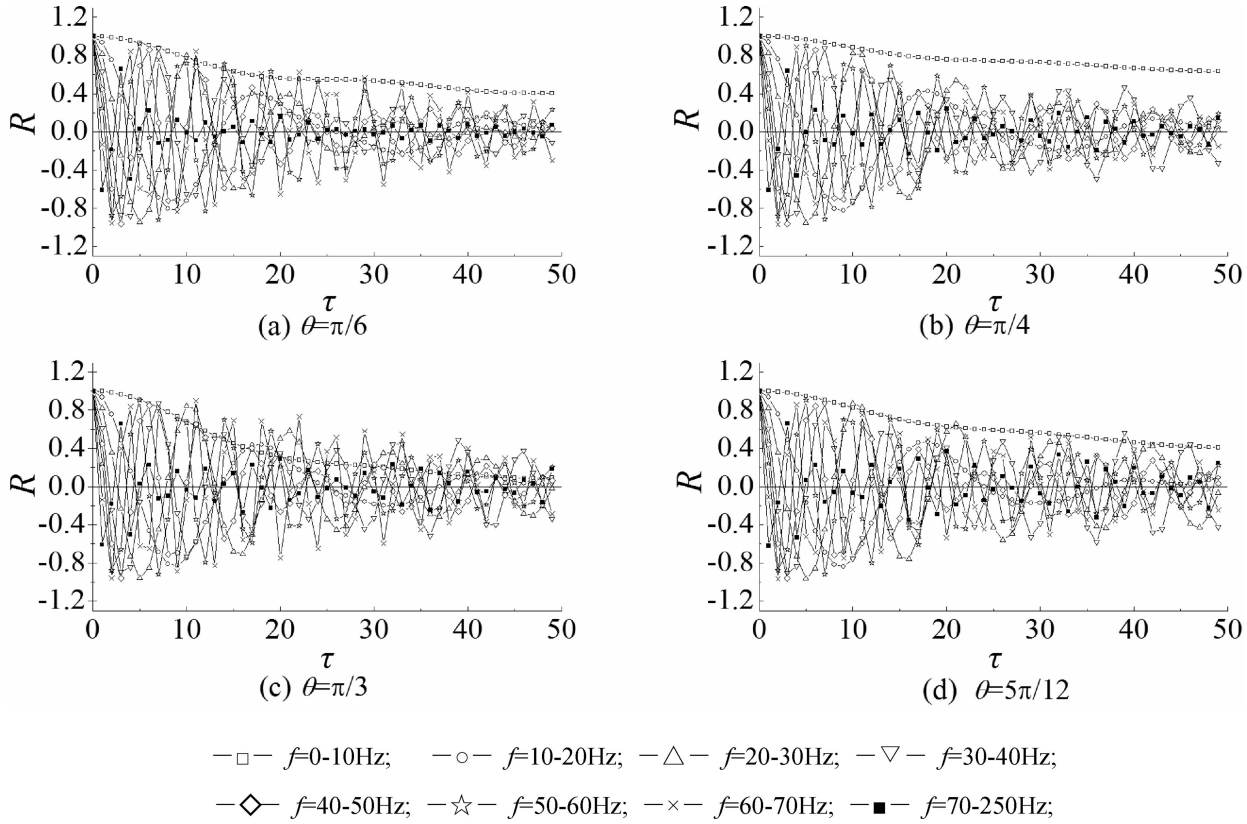

Fig. 5 – *Autocorrelation functions of decomposed time series with different frequency bands*

long-range correlation and random components. That is, PFS have chaotic characteristics. For a clear investigation, the instantaneous pressure time series at $Re = 32940$ were used as a case for analysis in subsequent sections.

Autocorrelation analysis

In order to examine the linear correlation of each decomposed component by Fourier filtering, their autocorrelation functions were calculated in detail as shown in Fig. 5. When the autocorrelation function firstly approaches zero, there is a linear correlation between time series signal $x(i)$ and its delay signal $x(i+\tau)$. The optimal time delays τ decrease with the increasing minimum of decomposed frequency bands at different circumferential positions for $z/H = 0.85$. The results show that the larger are the optimal time delays of fluctuation components, the weaker are the linear correlations.

Fig. 6 depicts the profiles of time delay intervals τ_a when the corresponding autocorrelation coefficients are firstly approximate to zero. For the frequency bands of 50–60 Hz and more than 60 Hz, the time delay intervals τ_a of decomposed fluctuation components are both 1 at different circumferential angles. It turns out that the signals of frequency above 50 Hz have no linear correlation in the time domain.

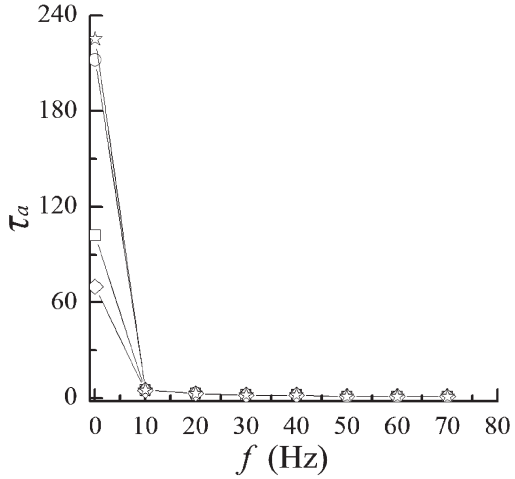

Fig. 6 – *Relationship between delay time of autocorrelation functions and lower limits of decomposed frequency bands*

Mutual correlation analysis

Autocorrelation functions could only examine the linear correlation between two time series, and the pressure fluctuations in the CJT have nonlinear chaotic behavior, displayed by Fig. 4. Therefore, the mutual information function is used to study the nonlinear correlation of PFS with different bands in

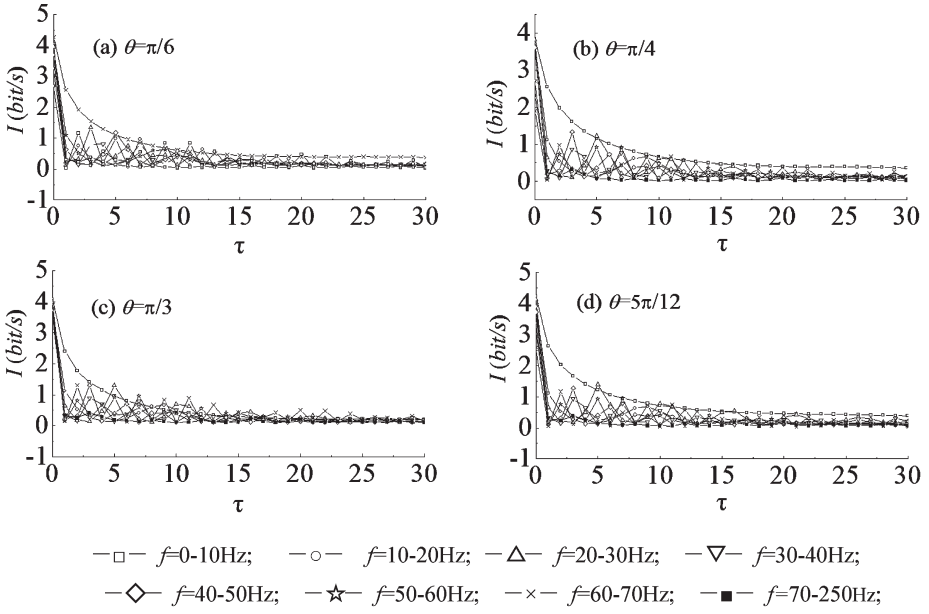

Fig. 7 – *Mutual information functions of decomposed time series with different frequency bands*

frequency under different circumferential angles. The relationship between the mutual information functions and the time delay intervals is shown in Fig. 7. As the lower limits of frequency bands increase, both the nonlinear correlation and time delay intervals τ_m decrease. The changing rate of mutual information with the decreasing time delay is the loss rate of the information and denotes the decreasing rate of predictability according to the physical meaning of mutual information. This shows that the randomness of the fluctuation signals increases and the nonlinear correlations weaken with the increasing lower limits of frequency bands.

As shown in the Fig. 8, the time delay intervals τ_m of PFS with different frequency bands are evaluated by mutual information functions. The results show that the signals of frequency above 60 Hz

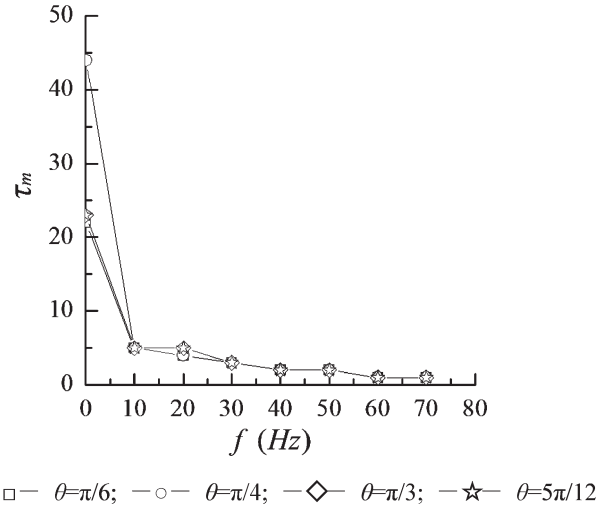

Fig. 8 – *Profiles of delay time of mutual information functions under the different lower limits of frequency bands*

do not have nonlinear correlation in the time domain. Therefore, they are considered as random signals. Comparing Fig. 6 and Fig. 8, the signals of 50–60 Hz in the frequency domain only have nonlinear correlation but do not have linear correlation. It could be concluded from Fig. 5 and Fig. 7 that PFS of 0–10 Hz have strong linear and nonlinear correlations because of the coupling interaction between large-scale forced and free vortexes in the CJT. The Rankine Vortex is formed due to the shear and entrainments among the multi jets with higher speed and the circumferential bulk fluid.

The profiles of autocorrelation and mutual information functions indicate that correlation exists in lower frequency band with larger scale fluctuations. In addition, the time delay intervals for the 0–10 Hz signals are different under different circumferential angles. For $\theta = \pi/6$, the fluid flow initializes at a beginning sector of jet and the velocity is nearly the same at different times, so the correlation is weaker. For $\theta = \pi/3$, the momentum decays quickly for the jet in the main sector and the time delay interval is the lowest among four measurement angles. Measurement points are far from the jet nozzle and near the tank wall at $\theta = 5\pi/12$, the radial secondary flow is induced by the coupling between baffles and jet flow and generates the strongest correlation of PFS.

However, the decomposed pressure fluctuation components with frequency above 10 Hz have similar optimized time delays in the CJT under different polar angles. These pressure fluctuation components come from the pulsation of smaller scales vortexes and the other fluid micelles. The dynamic characteristics are dominated by the large scale fluctuations with 0–10 Hz, and the contributions of

fluctuation components with frequency above 60 Hz to correlation are almost negligible.

Pressure fluctuations are very complicated. Pressure signals registered at any single location of the CJT consist of fluctuations induced by coupled interaction among the local vortexes with higher frequency, meso-scale and macro-scale vortexes. We begin to get a good knowledge of multi-scale flow characteristics in the CJT based on the studies of PFS. It will be useful for us to adjust and control the corresponding fluctuation components by optimizing the geometric constructions of the baffles, raisers and downcomer. On the other hand, the mixing efficiency will be improved.

Conclusion

The time delay correlations of PFS with different frequency bands were studied using autocorrelation and mutual information functions. The results are shown below:

With the increase in the time delays, the autocorrelation function of the original PFS decreases quickly and then fluctuates near zero. It could be seen from the profiles of different scales PFS that the fluctuations amplitudes, linear and nonlinear correlations decrease as the lower limits of decomposition frequency bands increase.

The PFS of frequency above 50 Hz are confirmed to be not linear independent and the signals above 60 Hz are not nonlinear independent at any time delay. Therefore, the signals of frequency above 60 Hz could be considered as random noise. Therefore, the pressure fluctuation components of less than 0–60 Hz are beneficial to mixing performances and should be extracted for further chaos nonlinear analysis. The profiles of time delay intervals under different circumferential angles are discussed. The dynamic characteristics are dominated by the large scale fluctuations with 0–10 Hz and the sequence from strong to weak of the correlation is at $5\pi/12$, $\pi/4$, $\pi/6$ and $\pi/3$.

ACKNOWLEDGMENT

The authors acknowledge funding support for this research from the National Natural Science Foundation of China (No. 21106086, No. 21306115), the Program for Liaoning Excellent Talents in University (No. LJQ2012035), the Science Foundation for Doctorate Research at Liaoning Science and Technology Bureau of China (No. 20131090) and the Science and technology research project of Liaoning Provincial Committee of Education (No.L2013164). We thank the referee for an enlightening remark that helped us improve the manuscript.

References

1. *Patkar, V. C., Patwardhan, A. W.*, Chem. Eng. Res. Des. **89** (2011) 904.
2. *Dakshinamoorthy, D., Louvar, J. F.*, Chem. Eng. Sci. **63** (2008) 2283.
3. *Pani, B. S., Patil, L. G.*, J. Hydro-Environ. Res. **1** (2007) 20.
4. *Wasewar, K. L.*, Chem. Biochem. Eng. Q. **20** (2006) 31**.**
5. *Zughbi, H. D., Rakib, M. A.*, Chem. Eng. Commun. **189** (2002) 1038.
6. *Hassel, E., Jahnke, S., Kornev, N., Tkatchenko I., Zhdanov, V.*, Chem. Eng. Sci. **61** (2006) 2908.
7. *Dong, L. L., Cheung, C. S., Leung, C. W.*, Int. J. Heat Mass Transfer **50** (2007) 5124.
8. *Icardi, M., Gavi, E., Marchisio, D. L., Barresi, A. A., Olsen, M. G., Fox, R. O., Lakehal, D.*, Chem. Eng. J. **166** (2011) 294.
9. *Nunes, M. I., Santos, R. J., Dias, M. M., Lopes, J. C. B.*, Chem. Eng. Sci. **74** (2012) 276.
10. *Yu, Y. F., Wu, J. H., Meng, H. B.*, Can. J. Chem. Eng. **89** (2011) 460.
11. *Yu, Y. F., Liu, X. R., Wu, J. H., Meng, H. B.*, Appl. Mech. Mater. **26/28** (2010) 382.
12. *Yu, Y. F., Meng, H. B., Wu, J. H.*, CFD model for optimum geometry design of a novel static jet mixer, ICCET, 2010.
13. *Meng, H. B., Yu, Y. F., Wu, J. H.*, Numerical simulation of the flow characteristic with different geometrical jet, ICIC, 2010.
14. *Zhang, W. H., Li, X. G.*, Chem. Eng. Sci. **64** (2009) 1009.
15. *Zheng, Y., Rinoshika, A., Yan, F.*, Chem. Eng. Sci. **72** (2012) 94.
16. *van der Schaaf, J., van Ommen, J. R., Takens, F., Schouten, J. C., van den Bleek, C. M.*, Chem. Eng. Sci. **59** (2004) 1829.
17. *Hsiaotao, T. B.*, Chem. Eng. Sci. **62** (2007) 3473.
18. *Hu, L. S., Wang, X. J., Yu, G. S., Wang, Y. F., Zhou, Z. J., Wang, F. C., Yu, Z. H.*, Nonlinear Anal. **10** (2009) 410.
19. *Tao, M., Jin, B. S., Zhong, W. Q., Yang, Y. P.*, Chem. Eng. Process **49** (2010) 340.
20. *Fan, L. S., Satija, S., Wisecarver, K.*, AlChE J. **32** (1986) 338.
21. *Fan, L. T., Neogi, D., Yashima, M., Nassar, R.*, AlChE J. **36** (1990) 1529.
22. *Vial, C., Camarasa, E., Poncin, S., Wild, G., Midoux, N., Bouillard, J.*, Chem. Eng. Sci. **55** (2000) 2957.
23. *van Ommen, J. R., Sasic, S., van der Schaaf, J., Gheorghiu, S., Johnsson, F., Coppens, M. O.*, Int. J. Multiphase Flow **37** (2011) 403.
24. *Cover, T. M., Thomas, J. A.*, Elements of information theory, 2nd ed., Wiley-Interscience, 2006.
25. *Brillinger, D. R., Guha, A.*, J. Stat. Plan. Infer. **137** (2007) 1076.
26. *Fraser, A. M., Swinney, H. L.*, Phys. Rev. A. **33** (1986) 1134.
27. *Jiang, A. H., Huang, X. C., Zhang, Z. H., Li, J., Zhang, Z. Y., Hua, H. X.*, Mech. Syst. Sig. Process. **24** (2010) 2947.
28. *Meng, H. B., Wang, W., Wu, J. H., Yu, Y. F., Wang, F.*, Chem. Eng. Res. Des. **90** (2012) 1750.
29. *Yu, Y. F., Wu, J. H., Meng, H. B.*, Journal of Beijing University of Chemical Technology **39** (2012) 23.
30. *Wang, L. Y., Wei, D. H., Zhao, L. M.*, J. Comput. **7** (2012) 1104.